

Pronounced ductility in CuZrAl ternary bulk metallic glass composites with optimized microstructure through melt adjustment

Zengqian Liu, Ran Li, Gang Liu, Kaikai Song, Simon Pauly, Tao Zhang, and Jürgen Eckert

Citation: *AIP Advances* **2**, 032176 (2012); doi: 10.1063/1.4754853

View online: <https://doi.org/10.1063/1.4754853>

View Table of Contents: <http://aip.scitation.org/toc/adv/2/3>

Published by the [American Institute of Physics](#)

Articles you may be interested in

[Crystallization and thermophysical properties of Cu₄₆Zr₄₇Al₆Co₁ bulk metallic glass](#)

AIP Advances **3**, 112115 (2013); 10.1063/1.4832235

[Correlation between the microstructures and the deformation mechanisms of CuZr-based bulk metallic glass composites](#)

AIP Advances **3**, 012116 (2013); 10.1063/1.4789516

[Plasticity-improved Zr–Cu–Al bulk metallic glass matrix composites containing martensite phase](#)

Applied Physics Letters **87**, 051905 (2005); 10.1063/1.2006218

[Bulk metallic glass matrix composites](#)

Applied Physics Letters **71**, 3808 (1997); 10.1063/1.120512

[Modeling deformation behavior of Cu–Zr–Al bulk metallic glass matrix composites](#)

Applied Physics Letters **95**, 101906 (2009); 10.1063/1.3222973

[Deformation behavior of metallic glass composites reinforced with shape memory nanowires studied via molecular dynamics simulations](#)

Applied Physics Letters **106**, 211902 (2015); 10.1063/1.4921857

PHYSICS TODAY

WHITEPAPERS

MANAGER'S GUIDE

Accelerate R&D with
Multiphysics Simulation

READ NOW

PRESENTED BY

 COMSOL

Pronounced ductility in CuZrAl ternary bulk metallic glass composites with optimized microstructure through melt adjustment

Zengqian Liu,¹ Ran Li,^{1,a} Gang Liu,² Kaikai Song,³ Simon Pauly,³ Tao Zhang,^{1,b} and Jürgen Eckert^{3,4}

¹Key Laboratory of Aerospace Materials and Performance (Ministry of Education), School of Materials Science and Engineering, Beihang University, Beijing 100191, China
²State Key Laboratory for Mechanical Behavior of Materials, School of Materials Science and Engineering, Xi'an Jiaotong University, Xi'an, 710049, China

³IFW Dresden, Institute for Complex Materials, P.O. Box 27 01 16, D-01171 Dresden, Germany

⁴TU Dresden, Institute of Materials Science, D-01062 Dresden, Germany

(Received 28 June 2012; accepted 11 September 2012; published online 19 September 2012)

Microstructures and mechanical properties of as-cast $\text{Cu}_{47.5}\text{Zr}_{47.5}\text{Al}_5$ bulk metallic glass composites are optimized by appropriate remelting treatment of master alloys. With increasing remelting time, the alloys exhibit homogenized size and distribution of *in situ* formed B2 CuZr crystals. Pronounced tensile ductility of $\sim 13.6\%$ and work-hardening ability are obtained for the composite with optimized microstructure. The effect of remelting treatment is attributed to the suppressed heterogeneous nucleation and growth of the crystalline phase from undercooled liquid, which may originate from the dissolution of oxides and nitrides as well as from the micro-scale homogenization of the melt. Copyright 2012 Author(s). This article is distributed under a Creative Commons Attribution 3.0 Unported License. [<http://dx.doi.org/10.1063/1.4754853>]

I. INTRODUCTION

Although bulk metallic glasses (BMGs) exhibit unique mechanical properties, such as high strength and elastic strain limit,^{1,2} their application as structural materials is strongly limited by their low room temperature ductility and macroscopic strain softening.^{3,4} To circumvent these restrictions, BMG composites combining a glassy matrix with ductile crystalline phases have been developed in various systems.^{5–10} By properly adjusting the compositions and microstructures, improved toughness and plasticity can be readily obtained in the composites under compressive or even tensile conditions.^{7,8} However, the combination of pronounced tensile ductility and macroscopic work-hardening ability was not obtained until the introduction of a B2 CuZr phase into the amorphous matrix in CuZr-based BMG composites.^{9–12} The prominent mechanical properties of the composites which originate mainly from the martensitic transformation of B2 CuZr to the B19' phase make them promising candidates for practical applications as high-performance structural materials.^{10–15}

Due to the large temperature gradient and cooling rate variation across the samples during the casting process, the size and distribution of *in situ* formed B2 CuZr crystals are typically non-uniform throughout the composites.^{12–15} This deteriorates the mechanical properties and the reliability of the composites, especially under tensile conditions. An effective adjustment of the microstructure is nevertheless essential because of the strong structural dependence of their mechanical properties.^{14,15} However, this ought to be quite challenging in such composites. On the one hand, the B2 CuZr phase forms by polymorphous crystallization from the melt which is different from the primarily

^aCorresponding author: E-mail: liran@buaa.edu.cn (R. Li);

^bzhangtao@buaa.edu.cn (T. Zhang); Tel/Fax: +86-10-82339705



precipitated beta dendrites in the Vit-type BMG composites.⁸ Thus the semi-solid processing method which utilizes the temperature span between the solidification points of crystalline phase and glassy matrix may not be adopted.⁸ On the other hand, rather high cooling rates are still required for the glass formation of the matrix upon casting, leaving just a short time window for the operational treatment.^{2,12} In addition, the crystal precipitation is very sensitive to the temperature and alloy compositions.^{13,16} So far, the desired control and adjustment of crystal nucleation and growth upon solidification has rarely been achieved in the composites except for an inoculation strategy proposed very recently.¹⁷ Considering the high susceptibility of the crystallization behavior of the undercooled melt to its thermal history, an appropriate melt treatment can be a potent measure for this processing.^{18–20}

In this study, we report a simple but effective method to properly adjust the microstructure and the mechanical properties of CuZr-based BMG composites using a remelting treatment. The origins of the effect are investigated from the viewpoint of thermodynamics and kinetics for crystallization of the B2 CuZr phase.

II. EXPERIMENTAL

Alloy ingots (~40 g for each sample) with nominal composition of $\text{Cu}_{47.5}\text{Zr}_{47.5}\text{Al}_5$ were prepared by are-melting the pure constituents (purity 99.5~99.99 wt.%) in Ti-gettered high-purity argon atmosphere. The ingots were remelted for 4, 8, 12 and 20 times, respectively, with ~1 min duration for each time under a fixed melting current of 410 A. The oxygen and nitrogen contents in the alloy ingots were measured by the inert gas fusion technique using a LECO-TC436 O/N analyzer with an error of less than 10%. The master alloys were then remelted in a quartz tube and injected under the same pressure into copper molds with cylindrical cavities of 3 mm diameter. The casting temperatures were kept almost constant for all the alloys with deviations of less than 50 K. For comparison, amorphous ribbons with a thickness of ~30 μm and a width of ~1 mm were prepared by melt spinning. The microstructures of the as-cast rods were analyzed by X-ray diffraction (XRD) and scanning electron microscopy (SEM). Tensile tests were performed on specimens with a gauge dimension of Φ 1.5 mm \times 6 mm machined from the Φ 3 mm rods at a strain rate of $3 \times 10^{-4} \text{ s}^{-1}$ at room temperature. The morphologies of the tensile fractured samples were characterized by a high-resolution SEM equipped with a field emission gun. The crystallization behavior of the glassy ribbons was examined using a differential scanning calorimeter (DSC) at a heating rate of 0.167 K/s. Isothermal annealing at temperatures of 708, 713, and 718 K, respectively, was also carried out in the DSC. The melting and solidification behavior was analyzed at a constant rate of 0.33 K/s using the ingots.

III. RESULTS AND DISCUSSION

Figure 1 shows the typical microstructures of the as-cast Φ 3 mm rods for the alloys remelted for different times. The central regions used for the tensile tests are marked by dashed circles. Crystalline particles in different morphologies and distributions are embedded in the amorphous matrix for all the alloys. The crystals were identified as the B2 CuZr phase by XRD (results not shown here). For the sample remelted for 4 times, a gradient microstructure was observed with the crystalline volume fraction and particle size decreasing radially from the center to the surface of the rod. The crystals are severely impinged in the center. In addition, coarse grains tend to precipitate in the sample with a dendrite substructure resolvable by SEM, as indicated by the white arrow in Fig. 1(a). The non-uniform features concerning the size and distribution of the B2 CuZr precipitates agree well with the widely reported results typically observed for CuZr-based BMG composites.^{12–15} With increasing remelting time, the samples exhibit lower volume fractions of B2 CuZr phase and reduced crystal sizes, pointing to an improved glass-forming ability (GFA) of the alloys. Furthermore, the distribution of the crystals is effectively homogenized by the remelting treatment. An optimized composite structure with ~13-75 μm large B2 CuZr crystals that are homogeneously distributed within the continuous glassy matrix is obtained after 12 times remelting. The average inter-particle spacing is ~53 μm . For the alloy remelted for 20 times, however, the crystalline volume fraction

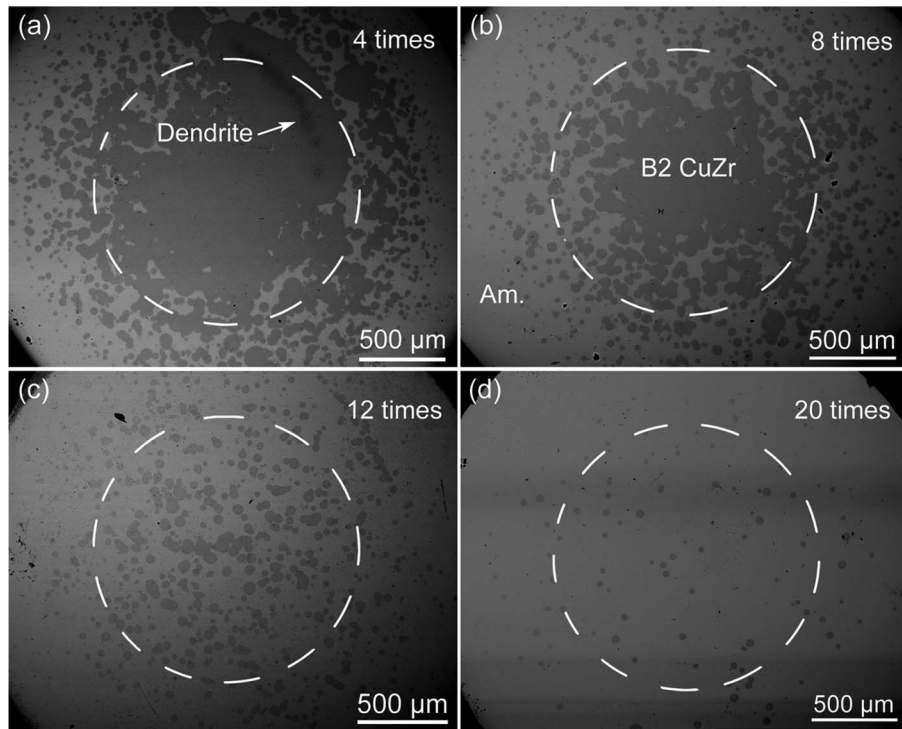


FIG. 1. SEM images of the as-cast 3 mm diameter BMG composites for the alloys remelted for different times. The central region used for the tensile tests is marked by a dashed circle for each sample.

becomes too low despite of the uniform distribution, which is expected to be deleterious to the mechanical properties of the composites.^{14,15}

The mechanical properties of the composites were evaluated by tensile tests on the dog-bone shaped samples. As shown in Fig. 2, the samples exhibit distinct tensile properties with the increase in remelting time. The longer the remelting time, the higher is the yield strength and the less pronounced is the work-hardening behavior of the composites. This can be attributed to the difference in microstructure, and mainly corresponds to the volume fractions of the B2 CuZr phase. As demonstrated by Pauly *et al.*, the compressive yield strength of the composites, which can be evaluated by either the rule of mixtures or the load-bearing model depending on the crystalline volume fraction present in the material, decreases quickly with an increase in the volume fraction of B2 CuZr phase.^{14,15} Based on our results, this trend is applicable to the tensile conditions although further more detailed analysis is required to validate the quantitative relations. On the other hand, as the work-hardening ability originates mainly from the martensitic transformation of B2 CuZr to the B19' phase,¹⁰⁻¹⁵ the crystalline volume fraction should be a key factor governing the work-hardening behavior of such composites. The work-hardening ability is expected to increase monotonically with the increase in B2 CuZr volume fraction, which is consistent with the results obtained by compression tests.^{14,15} Furthermore, the tensile ductility of the composites shows a strong dependence on the remelting time as well, but in a different manner. With increasing remelting time, the samples first exhibit both improved plastic strain and enhanced strength. The tensile ductility reaches a maximum value ($\sim 13.6\%$) for the 12-times-remelted alloy. The yield strength and average strain-hardening exponent of the sample are ~ 1190 MPa and ~ 0.25 , respectively. The tensile ductility and work-hardening ability of the composite are more pronounced while the yield strength is comparably high when compared with those of the reported BMG composites toughened by solid solutions or B2 CuZr phase.⁶⁻¹² For the alloy remelted for 20 times, however, only almost negligible ductility was found due to the high glassy volume fraction. These findings prove that the microstructure and mechanical properties of the composites can be effectively adjusted by controlling the remelting time of master alloys. An optimized combination of high yield strength, prominent tensile ductility,

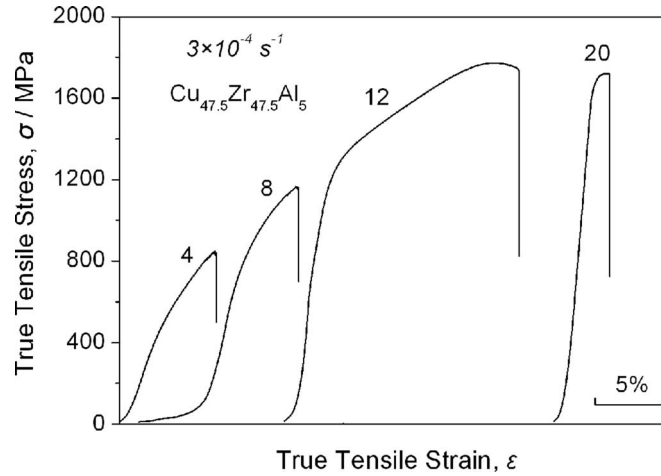


FIG. 2. True tensile stress-strain curves of the BMG composites for the alloys remelted for different times.

and pronounced work-hardening ability can be readily obtained in the as-cast alloys remelted for 12 times under the present conditions.

Figure 3 shows SEM images of a tensile fractured specimen for the 12-times-remelted alloy. The sample exhibits apparent necking just before the final fracture corresponding to the stress-drop segment on the stress-strain curve. Aside from the accumulation of shear bands in the necked region, a high density of multiple shear bands can be observed across the whole gauge section (Fig. 3(a)). During plastic deformation, the propagation of shear bands in the glassy matrix is hindered and arrested by the homogeneously dispersed crystalline precipitates, resulting in the multiplication of shear bands, as shown in Figs. 3(b)–3(d). Furthermore, through the martensitic transformation of the B2 CuZr phase, not only local stress concentrations at the two-phase interface are released,^{10–15} but also the applied strain can be accommodated by the ductile crystals.^{14,15} As the deformed crystalline particles which have experienced the transformation become harder than the undeformed regions,^{12,15} further plastic strain is accommodated by the undeformed crystals. The necking occurs only after nearly all the crystals have completed the transformation. Therefore, the sample exhibits a rather uniform plastic deformation along the whole gauge length after yielding. The restrained necking in the present sample indicates a significantly improved stability of plastic deformation in the composites.¹¹

It has been demonstrated that the plastic deformation in BMGs/BMG composites depends strongly on a characteristic plastic zone size R_p which can be expressed as

$$R_p = K_{IC}^2 / 2\pi\sigma_y^2, \quad (1)$$

where K_{IC} and σ_y are the plain-strain fracture toughness and the yield strength of the glassy matrix, respectively.^{2,3,8} Shear bands can be stabilized against developing into cracks by a second phase when the length-scale of the microstructural inhomogeneity L is smaller than but comparable to R_p in the composites.^{2,3,8} For the present CuZr-based metallic glass, R_p is estimated to be $\sim 240 \mu\text{m}$ by adopting the values of $K_{IC} \approx 70 \text{ MPa}\sqrt{\text{m}}$ and $\sigma_y \approx 1800 \text{ MPa}$.^{2,3,13} Therefore, the crystal size as well as the inter-particle spacing are both smaller than but of the same order of magnitude as R_p for the 12-times-remelted sample. This promotes the stabilization of shear bands and contributes to the enhanced tensile ductility. On the other hand, the fracture strain of the composites can be described as

$$\varepsilon_c = f_\alpha \varepsilon_\alpha + f_\beta \varepsilon_\beta + K f_{\alpha\beta} \varepsilon_{\alpha\beta}, \quad (2)$$

where ε_α , ε_β and $\varepsilon_{\alpha\beta}$ are the fracture strain of the single glassy phase, the crystalline phase and the ideal homogeneous “glassy + crystalline” composite, respectively. f_α , f_β and $f_{\alpha\beta}$ are the corresponding volume fractions of the three microstructural constituents, and K is a dimensionless

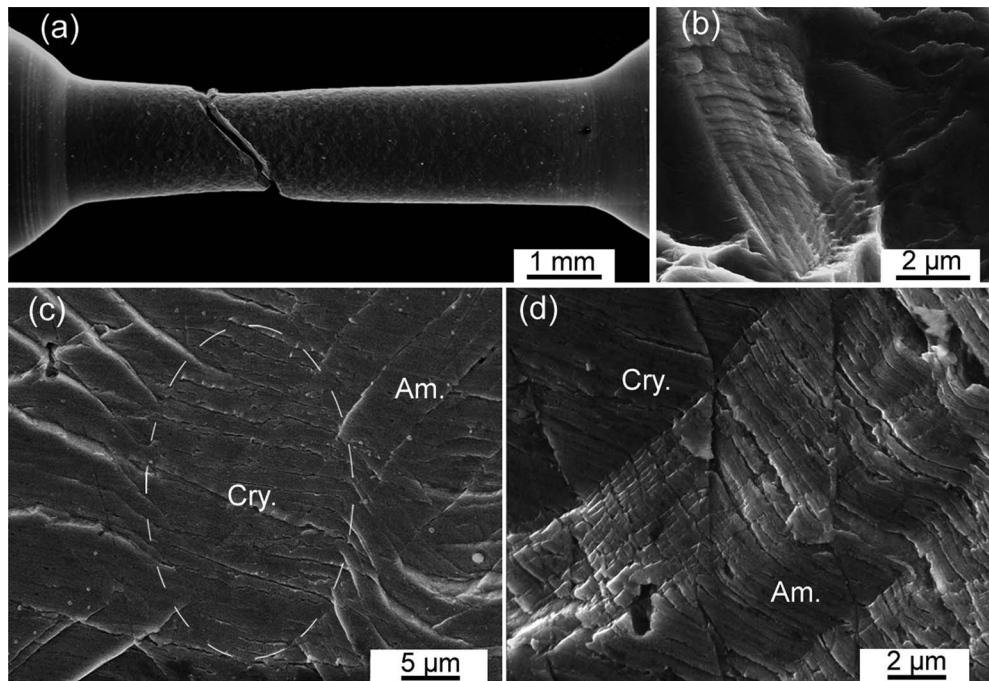


FIG. 3. Morphologies of the lateral (a, c, d) and fracture (b) surfaces of a tensile fractured sample for the alloy remelted for 12 times.

constant.^{14,15} Because $\varepsilon_{\alpha\beta}$ is much higher than ε_{α} and ε_{β} in tension, the homogenization in size and distribution of B2 CuZr particles which results in a larger $f_{\alpha\beta}$ for the same crystalline volume fraction will validly contribute to the tensile ductility of the composites. Therefore, the optimized microstructure with $f_{\alpha\beta}$ approaching 100 vol.% is very effective for obtaining the enhanced mechanical performance of the 12-times-remelted composites.

It is known that the thermodynamics and kinetics of crystallization from the undercooled melt are highly sensitive to inherent factors, such as inclusions, compositions and thermal history of the alloy.^{18–24} The structure and properties of cast alloys can be strongly affected by melt treatment.^{22–24} In this study, the varying trend of the microstructural features on the remelting time in the obtained BMG composites is definitely validated although the optimum remelting time may vary for different melting parameters and conditions. The effect of the remelting treatment may be understood from the following aspects. Firstly, inclusions such as refractory oxides and nitrides or oxygen/nitrogen stabilized phases may initiate heterogeneous crystal nucleation during the solidification process, especially in glass-forming systems.^{25–27} It has been reported that the detriments of oxides and other contaminants can be mitigated or eliminated by adopting remelting, overheating or successive heating-cooling thermal cycling treatments on the melt.^{18–27} In this study, the oxides and nitrides which may act as heterogeneous nucleation sites are expected to be broken down and dissolved by the remelting process. This can be manifested by the increased contents of oxygen and nitrogen measured for the remelted alloys, as shown in Fig. 4(a). The possibility of the contamination of leaked air into the arc-furnace can be ruled out because the oxygen tends to be saturated eventually. Thus the heterogeneous nucleation of B2 CuZr crystals is suppressed, contributing to the homogenization in the size and distribution of B2 CuZr particles as well as the improved GFA. Secondly, the benefits of minor doping of oxygen and nitrogen on the GFA have been validated in the CuZr-based alloys.^{16,28} It is reported that the dissolution of trace contents of oxygen and nitrogen in the liquid state can generate a wider atom size distribution and more efficient atomic packing structure in the alloys.^{16,28} As a result, the undercooled melt may exhibit a somewhat lower atomic diffusivity which leads to sluggish nucleation and growth kinetics of crystallization. This could give an explanation for the

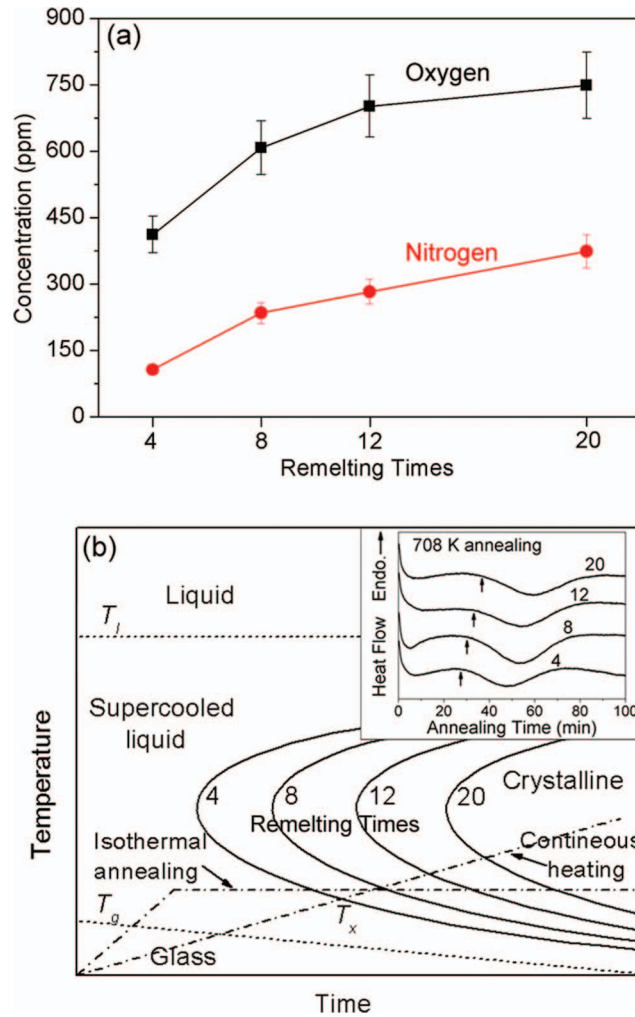


FIG. 4. Variation in the measured oxygen and nitrogen contents with remelting time (a) and schematic illustration of time-temperature-transformation diagrams for the alloys remelted for different times (b) with the isothermal annealing curves at 708 K shown in the inset.

improved GFA in the remelting treated alloys. Thirdly, micro-chemical or topological heterogeneities have been proved to exist in the alloy melts.^{18,24} The remelting treatment can result in the micro-scale homogenization of the melts, contributing to an enhanced GFA as well.^{18,19,29}

Therefore, by summing up the above discussion, the nucleation and growth of the B2 CuZr phase during solidification can be tuned or even suppressed by the remelting treatment, as illustrated in the schematic time-temperature-transformation diagram in Fig. 4(b). This trend is validated by the longer incubation time before crystallization with increasing remelting time, as shown in the inset and listed in Table I. For isothermal crystallization of the undercooled melt, the time needed to crystallize a small volume fraction x can be described as

$$t = \left(\frac{3x}{\pi I u^3} \right)^{1/4}, \quad (3)$$

where I and u denote the nucleation and growth rate of crystals, respectively.²⁹ Thus the increased incubation time can be attributed to the suppressed nucleation and growth of B2 CuZr crystals as elucidated above.

TABLE I. Thermal parameters, incubation times at different temperatures, and oxygen and nitrogen contents for the alloys remelted for different times. T_g is the glass transition temperature; T_x is the onset crystallization temperature; T_m is the melting temperature; T_l and T_s denote the liquidus temperature and onset solidification temperature, respectively.

Remelting Times	T_g (K)	T_x (K)	T_m (K)	T_l (K)	T_s (K)	ΔT_u = $T_l - T_s$ (K)	Incubation	Incubation	Incubation	O contents (ppm)	N contents (ppm)
							Time at 718 K (min)	Time at 713 K (min)	Time at 708 K (min)		
4	658	744	1140	1186	1163	23	8.2	17.1	27.4	412	107
8	655	744	1143	1187	1162	25	9.6	17.3	30.2	608	235
12	658	745	1140	1186	1158	28	9.3	18.2	33.2	702	283
20	655	746	1141	1187	1149	38	10.7	19.4	33.7	749	374

IV. CONCLUSION

In conclusion, the microstructure and mechanical properties of as-cast $\text{Cu}_{47.5}\text{Zr}_{47.5}\text{Al}_5$ BMG composites can be effectively adjusted by controlling the remelting time in the remelting treatment process. The longer the alloys are remelted, the smaller is the crystalline volume fraction and the more homogeneous are the size and distribution of B2 CuZr precipitates in the composites. For the present experiments, an optimized composite structure is obtained for the 12-times-remelted alloy which exhibits pronounced tensile ductility of $\sim 13.6\%$ and work-hardening ability. The heterogeneous nucleation and growth of crystals is suppressed by the remelting treatment, which can be attributed to the dissolution of oxides and nitrides as well as the micro-scale homogenization of the melt.

ACKNOWLEDGMENTS

This work was supported by the Natural Science Foundation of China (Grant Nos. 51071008 and 51131002), the National Basic Research Program of China (Grant No. 2010CB631003), the Innovation Foundation of BUAA for PhD Graduates and the Fundamental Research Funds for the Central Universities. One of the authors (K.K.S.) is grateful for the supported by the Chinese Scholarship Council (CSC), the National Basic Research Program of China (973 Program 2007CB613901), the National Natural Science Foundation of China (50831003 and 50631010), the Excellent Youth Project of the Natural Science Foundation of Shandong Province (JQ201012). Additional support (J.E.) was provided through the German Science Foundation under the Leibniz Program (Grant EC 111/26-1).

- ¹W. L. Johnson, *MRS Bull.* **24**, 42 (1999).
- ²G. Kumar, A. Desai, and J. Schroers, *Adv. Mater.* **23**, 461 (2011).
- ³M. F. Ashby and A. L. Greer, *Scripta Mater.* **54**, 321 (2006).
- ⁴Z. Q. Liu, R. Li, G. Wang, S. J. Wu, X. Y. Lu, and T. Zhang, *Acta Mater.* **59**, 7416 (2011).
- ⁵Y. Li, S. J. Poon, G. J. Shiflet, J. Xu, D. H. Kim, and J. F. Löffler, *MRS Bull.* **32**, 624 (2007).
- ⁶C. P. Kim, Y. S. Oh, S. Lee, and N. J. Kim, *Scripta Mater.* **65**, 304 (2011).
- ⁷C. C. Hays, C. P. Kim, and W. L. Johnson, *Phys. Rev. Lett.* **84**, 2901 (2000).
- ⁸D. C. Hoffmann, J. Y. Suh, A. Wiest, G. Duan, M. L. Lind, M. D. Demetriou, and W. L. Johnson, *Nature* **451**, 1085 (2008).
- ⁹S. Pauly, S. Gorantla, G. Wang, U. Kühn, and J. Eckert, *Nat. Mater.* **9**, 473 (2010).
- ¹⁰Y. Wu, Y. H. Xiao, G. L. Chen, C. T. Liu, and Z. P. Lu, *Adv. Mater.* **22**, 2770 (2010).
- ¹¹D. C. Hofmann, *Science* **329**, 1294 (2010).
- ¹²Y. Wu, H. Wang, H. H. Wu, Z. Y. Zhang, X. D. Hui, G. L. Chen, D. Ma, X. L. Wang, and Z. P. Lu, *Acta Mater.* **59**, 2928 (2011).
- ¹³S. Pauly, J. Bednarcik, U. Kühn, and J. Eckert, *Scripta Mater.* **63**, 336 (2010).
- ¹⁴S. Pauly, G. Liu, G. Wang, J. Das, K. B. Kim, U. Kühn, D. H. Kim, and J. Eckert, *Appl. Phys. Lett.* **95**, 101906 (2009).
- ¹⁵S. Pauly, G. Liu, G. Wang, U. Kühn, N. Mattern, and J. Eckert, *Acta Mater.* **57**, 5445 (2009).
- ¹⁶Z. Q. Liu, R. Li, H. Wang, and T. Zhang, *J. Alloys Compd.* **509**, 5033 (2011).
- ¹⁷Z. Q. Liu, R. Li, G. Liu, W. H. Su, H. Wang, Y. Li, M. J. Shi, X. K. Luo, G. J. Wu, and T. Zhang, *Acta Mater.* **60**, 3128 (2012).
- ¹⁸Y. J. Kim, R. Busch, W. L. Johnson, A. J. Rulison, and W. K. Rhim, *Appl. Phys. Lett.* **65**, 2136 (1994).
- ¹⁹L. Zhang, Y. S. Wu, X. F. Bian, S. Wu, and H. Li, *J. Mater. Sci. Lett.* **18**, 1977 (1999).
- ²⁰J. Schroers and W. L. Johnson, *J. Appl. Phys.* **88**, 44 (2000).

- ²¹ S. Mukherjee, Z. Zhou, J. Schroers, W. L. Johnson, and W. K. Rhim, *Appl. Phys. Lett.* **84**, 5010 (2004).
- ²² A. J. Drehman, A. L. Greer, and D. Turnbull, *Appl. Phys. Lett.* **41**, 716 (1982).
- ²³ J. J. Wall, C. T. Liu, W. K. Rhim, J. J. Z. Li, P. K. Liaw, H. Choo, and W. L. Johnson, *Appl. Phys. Lett.* **92**, 244106 (2008).
- ²⁴ V. Manov, P. Popel, E. Brook-Levinson, V. Molokanov, M. Calvo-Dahlborg, U. Dahlborg, V. Sidorov, L. Son, and Y. Tarakanov, *Mater. Sci. Eng. A* **304**, 54 (2001).
- ²⁵ A. Gebert, J. Eckert, and L. Schultz, *Acta Mater.* **46**, 5475 (1998).
- ²⁶ X. H. Lin, W. L. Johnson, and W. K. Rhim, *Mater. Trans. JIM* **38**, 473 (1997).
- ²⁷ L. Q. Xing and D. M. Herlach, *J. Mater. Sci.* **34**, 3795 (1999).
- ²⁸ Y. X. Wang, H. Yang, G. Lim, and Y. Li, *Scripta Mater.* **62**, 282 (2012).
- ²⁹ J. Schroers and W. L. Johnson, *Appl. Phys. Lett.* **76**, 234 (2000).